Thermal effects of hydrothermal circulation and seamount subduction: Temperatures in the Nankai Trough Seismogenic Zone Experiment transect, Japan

G. A. Spinelli

Earth and Environmental Science Department, New Mexico Institute of Mining and Technology, Socorro, New Mexico 87801, USA (spinelli@nmt.edu)

R. N. Harris

College of Oceanic and Atmospheric Sciences, Oregon State University, Corvallis, Oregon 97331, USA

[1] We examine the thermal effects of seamount subduction. Seamount subduction may cause transient changes in oceanic crust hydrogeology and plate boundary fault position. Prior to subduction, seamounts provide high-permeability pathways between the basaltic crustal aquifer and overlying ocean that can focus fluid flow and efficiently cool the oceanic crust. As the seamount is subducted, the high-permeability pathway is closed, shutting down the advective transfer of heat. If significant fluid flow occurs, it would be restricted after seamount subduction and would result in a redistribution of heat warming the trench and cooling landward parts of the system. Additionally, subducting seamounts can influence the position of the plate boundary fault that has thermal consequences by locally controlling the proportions of incoming sediment that subduct and accrete. Shifting the décollement to the seafloor at the trench in the wake of seamount subduction causes limited cooling focused at the toe of the margin wedge. We apply these features of seamount subduction to a thermal model for the Nankai Trough Seismogenic Zone Experiment transect on the margin of Japan. Models with hydrothermal circulation provide an explanation for anomalously high surface heat flux observations near the trench. They yield temperatures of ~100°C−295°C for the rupture area of the 1944 Tonankai earthquake. Temperatures in the region of episodic tremor and slip are estimated at ~290°C–325°C, ~70°C cooler than a model with no fluid circulation.

1. Introduction

[2] Seamounts approaching and entering a subduction zone likely modify the thermal state of the region. Seamounts are an important control on the thermal state of oceanic lithosphere due to their influence on hydrothermal circulation [*Villinger et al.*, 2002; *Fisher et al.*, 2003b; *Fisher and Wheat*, 2010]. Seamounts and other basement outcrops provide high-permeability regions of recharge or discharge, influencing region-scale fluid circulation that can affect the thermal state of surrounding oceanic crust [*Mottl et al.*, 1998; *Fisher et al.*, 2003a, 2003b; *Harris et al.*, 2004; *Hutnak et al.*, 2006, 2008; *Wheat and Fisher*, 2008]. "Ventilated" fluid circulation, where fluids freely circulate between the ocean and the crust, can efficiently cool oceanic lithosphere, locally decreasing the heat content of the plate. This ventilated circulation occurs as fluids circulate laterally between basement outcrops that serve as regions of recharge and discharge. If fluid flow velocities are sufficient for efficient heat extraction, the oceanic lithosphere is cooled. Sediment cover acts as a low-permeability cap to flow within the underlying basaltic basement of oceanic crust [*Spinelli et al.*, 2004]. Where sedimentary cover inhibits the advective heat exchange between the basaltic basement aquifer and the ocean, "insulated" flow conditions in the underlying basaltic basement exist [*Fisher*, 2004].

[3] Individually, both ventilated and insulated patterns of heat transfer in oceanic lithosphere can have a profound impact on the thermal state of a subduction zone. Offshore Cape Muroto on the Nankai margin of southern Japan, insulated hydrothermal circulation in the incoming and subducting oceanic crust efficiently transfers heat from the deeper subduction zone to the trench and incoming plate [*Spinelli and Wang*, 2008]. Offshore Costa Rica, the thermal state of the subduction zone in adjacent regions with and without prominent seamounts on the incoming plate are affected by ventilated and insulated hydrothermal circulation, respectively [*Harris et al.*, 2010]. As a fairly isolated seamount approaches then enters a subduction zone, the regional fluid flow regime may transition from ventilated to insulated circulation as the high-permeability conduit (i.e., seamount) between the basaltic basement aquifer and ocean is eliminated (i.e., subducted) from the system. This scenario has yet to be explored, but may apply to the well-studied NanTroSEIZE transect on the Nankai margin of Japan.

[4] In addition to their influence on the hydrothermal system, subducting seamounts disrupt the margin, leading to landslides and erosional embayments [*von Huene et al.*, 2000] as well as fracturing the overriding margin [*Wang and Bilek*, 2011]. Importantly for the thermal regime, seamount subduction may also transiently move the décollement upward, locally altering the ratio of accreting and subducting sediments. By moving the décollement upward, seamounts may locally increase the volume of subducting sediments and erode the upper plate from below [*Dominguez et al.*, 2000]. Because the recently deposited trench sediments are relatively cold, this effect may also cool the shallow subduction zone. The physical disruption of the margin wedge by seamount subduction may also alter the permeability structure of the wedge. The permeability of subduction zone faults [*Bekins et al.*, 1995; *Fisher et al.*, 1996; *Saffer and Bekins*, 1998; *Screaton et al.*, 2000] is typically 4–8 orders of magnitude lower than the permeability of the basaltic basement aquifer of oceanic crust [*Becker and Davis*, 2004]. However, transient increases in fault zone permeability are possible [e.g., *Bekins et al.*, 1995; *Saffer and Bekins*, 1998], and associated transient pulses of fluid flow can advect heat [e.g., *Fisher and Hounslow*, 1990].

[5] We develop general thermal models to examine some of the thermal effects of seamount subduction. We examine the potential influence on ocean crust hydrogeology of a seamount approaching and entering the subduction zone. We also examine the thermal effect of moving the décollement position in response to seamount subduction. Finally, we model temperatures in the subduction zone in the NanTroSEIZE transect, including potential thermal effects of the recent subduction of a seamount in the region.

2. Geological Setting of the NanTroSEIZE Transect

[6] Along the Nankai margin, the Philippine Sea plate subducts beneath Japan at ∼4.6 cm yr^{-1} [*Seno et al.*, 1993]. Subduction along this margin has been active for the past ∼15 Ma [*Okino et al.*, 1994]. Magnetic lineations and oceanic lithosphere isochrons are roughly parallel to the convergence direction, perpendicular to the trench axis [*Okino et al.*, 1994]. The Nankai Trough Seismogenic Zone Experiment (NanTroSEIZE) transect is ∼200 km northeast of the axis of a fossil spreading center; currently, ∼20 million year old oceanic lithosphere

is subducting in this transect. The oceanic lithosphere subducting in the NanTroSEIZE transect has aged from ~5 Ma at the initiation of subduction to ~20 Ma today [*Okino et al.*, 1994]. At the deformation front, sediment on the incoming plate is ~2400 m thick [*Ike et al.*, 2008; *Moore et al.*, 2009]. Despite the thick incoming sediment section, currently all of the incoming sediment is subducting [*Moore et al.*, 2009]. In a global analysis, *Clift and Vannucchi* [2004] found that sedimentary accretion is favored in regions of slow convergence (<7.6 cm yr^{-1}) and thick sediments (>1 km). This complete sediment subduction is likely a recent phenomenon, as young sediment comprises the margin wedge in the NanTroSEIZE transect. Trench wedge facies sediment in the margin wedge is <1 million years old and material in the wedge interior is <6 million years old [*Expedition 316 Scientists*, 2009a, 2009b]. Subduction of all the incoming sediment on the NanTroSEIZE transect may result from local disruption of the margin by recent subduction of a seamount. Centered approximately 10 km southwest of NanTroSEIZE transect, a ~8 km wide landward indentation of the accretionary prism toe with a steep headwall is interpreted as a landslide scar probably caused by subduction of a small seamount (Figure 1b) [*Moore et al.*, 2009]. A small subducted seamount is imaged ~5 km landward of the trench in this location (on seismic reflection line ODKM03-I in the work by *Taira et al.* [2005]). Given the current convergence rate, this seamount impacted the margin wedge and began influencing local subduction and structural processes ~100,000 years ago. The rugged appearance of landslide debris deposits in the trench axis downslope of the scar [*Moore et al.*, 2009] is also consistent with recent (i.e., 100,000 years ago) seamount subduction and associated margin deformation. We infer that this seamount subduction may have caused a shift in décollement position to the seafloor at this time leading to the complete subduction of incoming sediment.

3. Regional Heat Flux Data

[7] Surface heat flux data are the primary observational constraint on subduction zone thermal models. The heat flux data along the NanTroSEIZE transect include: seafloor probe measurements [*Yamano et al.*, 2003; *Kinoshita et al.*, 2008; *Hamamoto et al.*, 2011], observations from Integrated Ocean Drilling Program (IODP) boreholes [*Kimura et al.*, 2008; *Harris et al.*, 2011], long-term temperature monitoring at continental shelf sites [*Hamamoto et al.*,

2005], estimates from the depth to a gas hydrate related bottom simulating reflector [*Kinoshita et al.*, 2011], and temperature gradients in boreholes on land [*Yamano et al.*, 2003].

[8] Along the entire Nankai margin, an anomalously "hot trench" has been a long-standing observation [*Yamano et al.*, 1984]. Similar to other parts of the margin, the incoming plate slightly seaward of the trench in the NanTroSEIZE transect is characterized by high heat flux (Figure 2) [*Watanabe et al.*, 1970; *Yamano et al.*, 1984, 2003; *Kinoshita et al.*, 2008]. Heat flux decreases landward of the trench, consistent with the subduction of low-temperature oceanic lithosphere relative to the overriding plate. Offshore Cape Muroto, heat flow seaward of the trench shows a prominent peak with values in excess of 250 mW m^{-2}. These values are significantly higher than conductive predictions (~110 mW m^{-2}) and exhibits variability characteristic of fluid flow. This peak in heat flow at the trench offshore Cape Muroto has been interpreted in terms of insulated fluid and heat circulation in subducting crust [*Spinelli and Wang*, 2008, 2009]. Sediment alteration on the incoming plate in the Muroto region is consistent with short-lived recent reheating of the incoming plate, associated with fluid circulation in the subducting crust; it is not consistent with anomalously warm lithosphere over millions of years [*Spinelli and Underwood*, 2005]. As with other parts of the Nankai margin, the trench in the NanTroSEIZE transect is anomalously warm (Figure 2) [*Harris et al.*, 2011]. Seafloor probe observations in the NanTroSEIZE transect are somewhat higher than heat flux determinations from IODP Expeditions 315 and 316 sites [*Hamamoto et al.*, 2011; *Harris et al.*, 2011]. The shallow probe data likely are influenced by bottom water temperature variations or by the transport of surface sediments; heat flux observations from the IODP sites provide a more robust constraint on the thermal state of the margin [*Harris et al.*, 2011].

4. Thermal Modeling Methods

[9] We use numerical models of heat production and transport in a subduction zone to examine the thermal effects of recent subduction of a small seamount. We focus on two aspects of seamount subduction: 1) a transient change in the depth to the plate boundary fault near the deformation front, and 2) a seamount on the incoming plate acting as a conduit for advective heat exchange between the oceanic lithosphere and the overlying ocean.
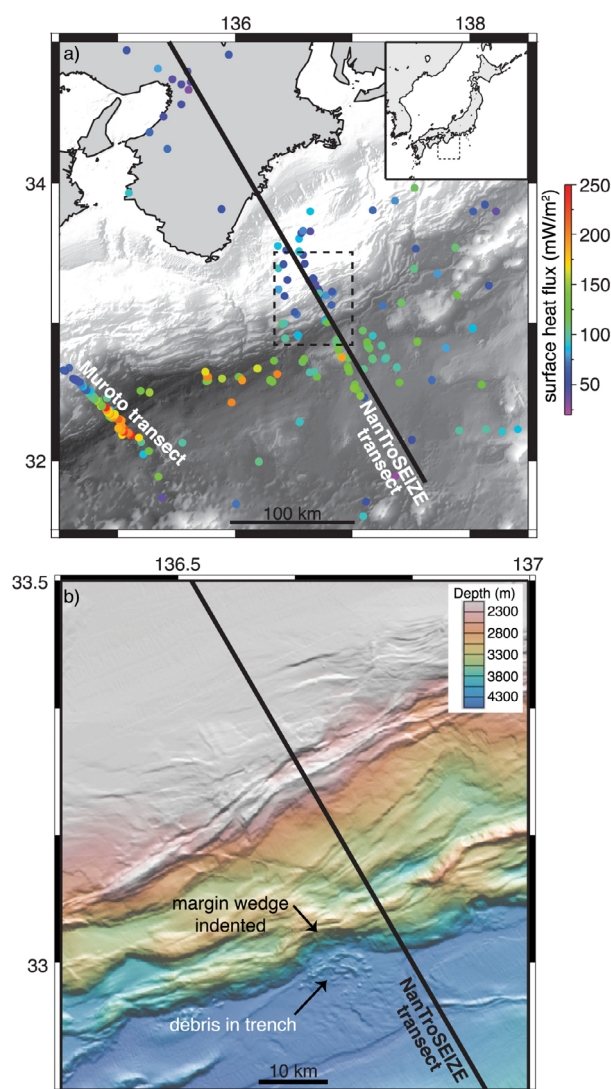
Figure 1. (a) Surface heat flux observations on the Nankai margin offshore southern Japan (inset shows location of study area) indicate a warm trench relative to the surrounding seafloor. We develop thermal models for the Nankai Trough Seismogenic Zone Experiment (NanTroSEIZE) transect along the bold line. Comparisons are made to the Muroto transect, where numerous heat flux observations cross the trench. (b) Centered ~10 km west of the NanTroSEIZE transect, the toe of the margin wedge is indented likely due to subduction of a seamount; blocky debris fills the trench. Dashed box in Figure 1a indicates area of detailed bathymetry shown in Figure 1b.

Examining each of these phenomena requires simulation of transient changes in the subduction zone thermal system. We use a transient 2-D finite element model [*Wang et al.*, 1995] to simulate temperatures in a cross section through a subduction zone. Because seamounts are 3-D features, our 2-D

approach exaggerates their thermal effect, but as we will show the thermal impact of the subducting seamount is small. On the Nankai margin, the seamount of interest is out of the plane of the NanTroSEIZE transect. The seamount itself is not modeled; we model the regional thermal effects of the seamount (i.e., the change in position of the décollement and the change in the hydrogeology). The model includes heat conduction, radiogenic and frictional heat production, and advection of heat with the subducting slab.

[10] First, we use a series of simulations to examine the general thermal effects of seamount subduction over a range of convergence rates and hydrogeologic scenarios, then we examine the specific case of the thermal state of the NanTroSEIZE transect. For all simulations we use a cross-section geometry based on that observed in the NanTroSEIZE transect; the geometry is derived from seismic reflection data for the shallow portion of the system [*Moore et al.*, 2009] and tomographic imaging for the deeper slab geometry [*Hirose et al.*, 2008]. Temperature at the upper boundary of the model is fixed at 0°C, and at the base of the oceanic lithosphere is fixed at 1400°C. At the landward boundary, we use a geotherm consistent with a back-arc setting; the landward boundary is far from the region of interest to avoid boundary effects. At the seaward boundary (150 km from the trench), we use a geotherm for 15 Ma conductively cooled oceanic lithosphere. We use an effective friction coefficient of 0.03, consistent with simulations for the Muroto transect [*Spinelli and Wang*, 2009] and numerous other subduction zone thermal models [e.g., *Wada and Wang*, 2009; *Harris et al.*, 2010]. Mechanical and thermal studies indicate that the average (temporally and spatially) effective friction coefficient is usually <0.05 [*Wang et al.*, 1995; *Wang and He*, 1999]. The distribution of physical properties is shown in Table 1; it follows models from the nearby Muroto transect [*Hyndman et al.*, 1995; *Wang et al.*, 1995; *Wang et al.*, 2004; *Spinelli and Wang*, 2008]. Thermal conductivity and heat capacity values are estimated from local values where available, or are typical values based on rock type [*Dumitru*, 1991; *Hyndman and Wang*, 1993]. Radiogenic heat production values are based on K, Th, and U data from the incoming sediment section [*Taira et al.*, 1991; *Hill et al.*, 1993] and from plutonic rocks in southwestern Japan [*Kanaya and Ishihara*, 1975]. *Hyndman et al.* [1995] provide an extensive review of uncertainty in thermal models for the Nankai margin resulting from variations in material properties, initial conditions, and margin
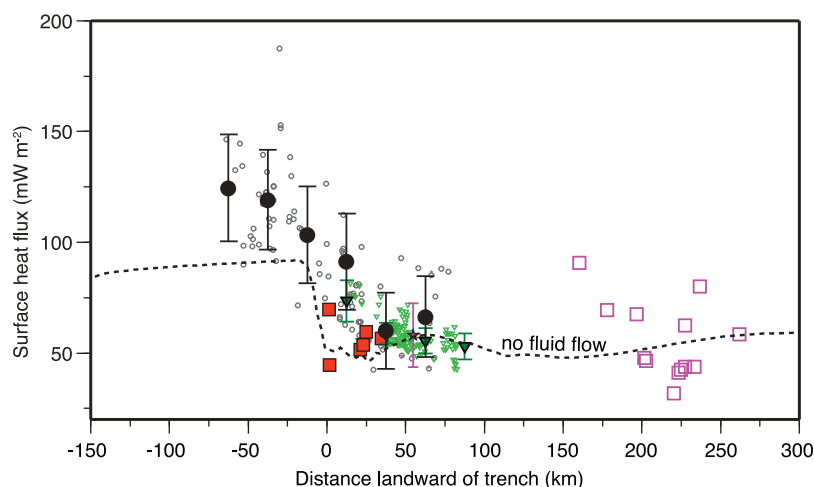
Figure 2. Observed and modeled surface heat flux along the NanTroSEIZE transect. Observations are from probe measurements (circles), ODP and IODP sites (solid squares), land boreholes (open squares), BSR estimates (inverted triangles), and long-term shelf measurements (stars). Observations within 50 km of the transect are shown. For probe, BSR, and long-term shelf observations, small symbols are individual measurements; large solid symbols are means for 25 km wide bins. Error bars are ±1 standard deviation. Dashed line is modeled surface heat flux with no fluid circulation in oceanic crust.

geometry; they estimate error bars of ±25°C on the 350°C and 450°C isotherms on the plate boundary fault.

[11] We examine three sets of models that increase in complexity. Our first set of simulations represents the reference model; we assume a static plate boundary fault position and no fluid flow. In this reference simulation the plate boundary fault is located such that 1400 m of incoming sediment is accreted and 1000 m of incoming sediment is subducted throughout the entire 20 Ma simulation (Figure 3a). In the second set of models we examine the effects of a recent shift in the location of the plate boundary fault attributed to seamount subduction. We simulate subduction with active accretion (1400 m of sediment accreting, 1000 m of sediment subducting), then shift the décollement to

the seafloor at the trench so all the sediment on the incoming plate subducts. Simulations are run to steady state prior to seamount subduction and an additional 5 Ma of simulation time after seamount subduction (Figure 3b). In both the reference simulation and the simulations with the temporal change in décollement position, we run simulations with convergence rates of 2.5, 5.0, and 10.0 cm yr^{-1}.

[12] In the third set of models, we include the effects of hydrothermal circulation in the basaltic basement of the oceanic lithosphere. In the extremely permeable upper basement rocks of oceanic crust, the efficiency of convective heat transfer is very high and the Nusselt number (Nu) can exceed 100 [*Davis et al.*, 1997; *Spinelli et al.*, 2004; *Kummer and Spinelli*, 2008; *Spinelli and Wang*, 2008]. In systems with hydrothermal circulation vigorous enough to have Nu in excess of 20, a high-conductivity proxy for the thermal effects of the fluid circulation is accurate [*Davis et al.*, 1997]. This inspired *Spinelli and Wang* [2008] to use such a proxy to adapt a general subduction zone thermal model to include the effects of vigorous circulation in the ocean crust aquifer. We use the same high-conductivity proxy in this study. Using this technique, the thermal effect of vigorous fluid circulation in the oceanic crust aquifer is simulated by increasing the thermal conductivity of the aquifer material. First, we calculate temperatures in the oceanic crust aquifer without enhanced thermal conductivity (i.e., with no effects of hydrothermal

Table 1. Thermal Model Parameters[a]

Unit	Thermal Conductivity (W m^{-1} K^{-1})	Heat Production (mW m^{-3})	Heat Capacity (J m^{-3} K^{-1})
Incoming sediment	1.25	1.9	2.5 × 10^6
Oceanic crust	2.9	0.02	3.3 × 10^6
Accreted sediment	1.5–2.5[b]	1.9–2.4[b]	2.5 × 10^6
Continental crust	2.5	0.4–2.4[c]	2.5 × 10^6
Mantle	3.1	0.02	3.3 × 10^6

[a]*Hyndman et al.* [1995].
[b]Conductivity and heat production increase linearly from toe of prism to backstop.
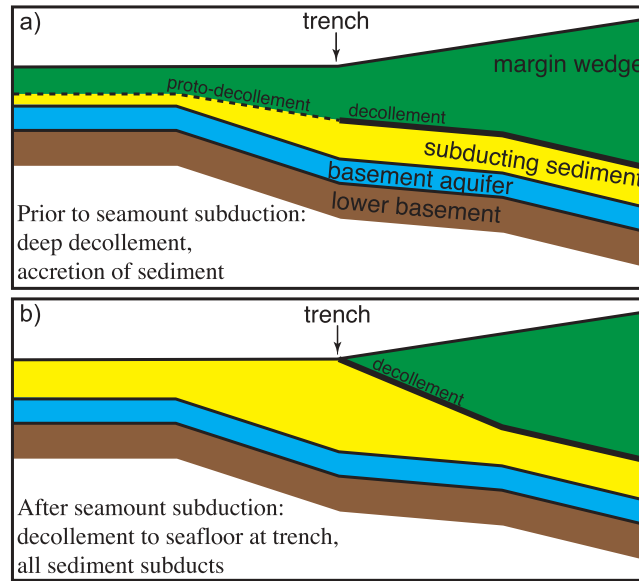[c]Heat production decreases linearly from 0 to 10 km depth.

Figure 3. Cartoon cross sections showing portion of model around the trench. Green shading is accreted and accreting sediment. Yellow shading is subducting sediment. Blue shading is 600 m thick aquifer in basaltic basement rock of oceanic lithosphere; the thermal effect of vigorous fluid circulation in the aquifer is simulated via a high thermal conductivity. Brown shading is lower oceanic lithosphere. (a) Accretion of sediment prior to influence of seamount subduction. (b) All sediment on the incoming plate is subducted.

circulation). We use the modeled temperatures, temperature-dependent fluid properties, and the heat flux into the base of the aquifer to calculate the Rayleigh number throughout the aquifer using:

$$Ra = \frac{\alpha g k L^2 \rho_f q}{\mu \kappa K}$$

where α is the fluid thermal expansivity, g is gravitational acceleration, k is aquifer permeability, L is aquifer thickness, ρ_f is fluid density, q is heat flux into the base of the aquifer, μ is fluid viscosity, κ is thermal diffusivity, and K is thermal conductivity [*Bessler et al.*, 1994]. The proportion of heat transported by convection increases as the vigor of convection increases; thus, the Nusselt number increases as the Rayleigh number increases. We estimate the Nusselt number (Nu) from the Rayleigh number (Ra) using:

$$Nu = 0.08 Ra^{0.89}$$

[*Wang*, 2004; *Spinelli and Wang*, 2008]. Finally, the thermal conductivity for each aquifer element is increased by a factor of Nu over the material conductivity. The conductive model is rerun with the updated aquifer thermal conductivities, yielding new aquifer temperatures. The process is repeated until the temperatures stabilize. In calculating Ra for the aquifer, we test three permeability versus depth

trends for the basement aquifer. One is the preferred trend derived from the Muroto transect,

$$k = 10^{-9.0-0.055z},$$

where z is aquifer depth below seafloor (km), which yields a presubduction aquifer permeability of 10^{-9} m^2, at the upper end of previous estimates for regional-scale permeability of the ocean crust aquifer [*Becker and Davis*, 2004; *Spinelli and Fisher*, 2004; *Hutnak et al.*, 2008]. The two additional permeability trends examined are lower, spanning the range of estimates for regional-scale oceanic crust aquifer permeability:

$$k = 5x10^{-10.0-0.055z}$$

and

$$k = 10^{-10.0-0.055z}.$$

[13] The upper oceanic crust aquifer is assumed to be continuous over 10s of km, consistent with observations of long-distance transport in the oceanic crust aquifer at other locations [*Fisher et al.*, 2003b; *Hutnak et al.*, 2006, 2008]. We do not consider the small fluid sources due to dehydration reactions in the slab. They are important for fluid flow only if the permeability is extremely low, in

which case the slow fluid flow is not thermally significant [Peacock, 1987, 1996].

[14] Except where the sediment cover is disrupted by bathymetric relief such as seamounts, low-permeability seafloor sediment hydraulically isolates the basaltic basement aquifer from the overlying ocean. In one subset of these simulations, we model insulated hydrothermal circulation where fluids are restricted to the basaltic basement aquifer, and in another subset of simulations we model ventilated fluid flow where fluids exchange freely between the ocean and the basement aquifer. In the ventilated models, we set the vertical temperature gradient to 20°C km^{-1} through the basement aquifer over a region 5 km wide that simulates the out of plane seamount. This thermal gradient is consistent with observations from well ventilated ~20 Ma oceanic lithosphere [Fisher et al., 2003a; Hutnak et al., 2008] and is significantly lower than the predicted vertical temperature gradient for conductively cooling 15 Ma lithosphere of ~70°C km^{-1} [Stein and Stein, 1994]. Thus, the net effect of the simulated seamount is to cool the surrounding lithosphere. In this model the convergence rate is 5.0 cm yr^{-1}. Upon entering the subduction zone, the seamount is buried, shutting off the hydrologic connection between the basement aquifer and the ocean. After seamount subduction, the aquifer supports insulated circulation. Simulations are run for 5 Ma after seamount subduction.

[15] In the final series of simulations, we apply these results to the NanTroSEIZE transect. First, we generate a reference simulation that excludes the impact of seamount subduction. Then, we examine the effects of the shift in décollement position to the trench for the final 0.1 Ma of simulation time. Finally, we explore the possible thermal effects of both insulated and ventilated hydrothermal circulation in the NanTroSEIZE transect. The convergence rate is 4.6 cm yr^{-1}, yielding a final seamount position 4.6 km landward of the trench. We use the highest aquifer permeability trend, consistent with results from the nearby Muroto transect. The incoming plate ages from 5 Ma lithosphere at the beginning of the simulation to 20 Ma lithosphere at the end.

5. Results

[16] The reference thermal model with a constant décollement position and no fluid circulation in the oceanic crust yields modeled surface heat flux of ~95 mW m^{-2} on the incoming plate and ~60 mW

m^{-2} on the margin wedge (Figure 4). Surface heat flux drops as the incoming plate is rapidly buried and subducted, advecting cold near-seafloor material down into the system. In the second set of models, we shift the position of the plate boundary fault to the seafloor at the trench for the last 5 Ma of the simulation so that cold surface sediments are transported under the toe of the margin wedge. The shift in the plate boundary fault suppresses surface heat flux by <15 mW m^{-2} in an area restricted to within ~5 km of the trench. The effect scales with the convergence rate, decreasing ~6 mW m^{-2} for the slowest convergence rate and ~13 mW m^{-2} for the fastest convergence rate examined. Most of the thermal effect on the surface heat flux pattern is realized by 100,000 years after the shift in décollement position (Figure 4).

[17] In simulations that include insulated hydrothermal circulation, the basaltic basement aquifer facilitates long-distance lateral heat transport in a 600 m thick zone beneath the sedimentary cover and the margin wedge. Heat is transported in the aquifer from deep in the subduction zone to the shallow part of the system and the incoming plate. Relative to a simulation without vigorous heat transport in the aquifer, surface heat flux is lower on the margin wedge and higher on the incoming plate with a spike in heat flux ~10 km seaward of the trench (Figure 5). For the lowest aquifer permeability, the spike in surface heat flux reaches 116 mW m^{-2} (~20 mW m^{-2} above the no fluid flow case). For the highest aquifer permeability, the maximum surface heat flux is 137 mW m^{-2}. The maximum reduction in heat flux on the margin wedge ranges from 4 to 10 mW m^{-2}, the largest effect occurring with the highest aquifer permeability.

[18] In the set of simulations with a transition from ventilated to insulated hydrothermal circulation due to seamount subduction, the seamount on the incoming plate extracts heat from the surrounding lithosphere. The cooled region around the seamount increases in size with increasing aquifer permeability (Figure 6). After the seamount subducts, fluid circulation in the basement aquifer continues, but advection from the aquifer to the ocean is shut off; heat is only redistributed within the aquifer below the seafloor sediments. Thus, the thermal state of the subduction zone after seamount subduction gradually approaches that achieved in the insulated hydrothermal circulation case. Within 500,000 years after seamount subduction, surface heat flux on the incoming plate recovers to levels near those for the reference (no fluid flow) case.
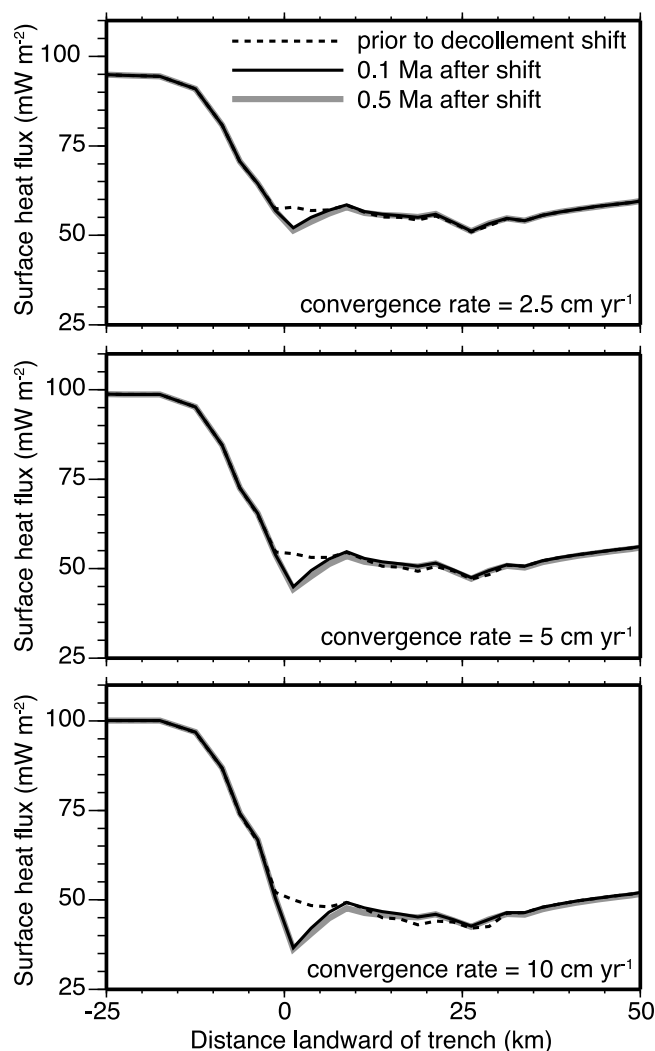
Figure 4. Effects of switching décollement position on surface heat flux near the trench. Dashed line is modeled surface heat flux with constant plate boundary fault position throughout simulation. Thin black line is modeled surface heat flux 100,000 years after shifting plate boundary fault to trench (i.e., subduction of all incoming sediment); bold gray line is 500,000 years after shift in décollement position.

By 5 Ma after seamount subduction, the magnitude of the trench heat flux spike is 67% of the anomaly in the insulated circulation case for the lowest permeability. With the highest permeability, the magnitude of the trench heat flux spike at 5 Ma after seamount subduction is 85% of that in the insulated circulation case (Figure 6).

[19] For the simulations of the NanTroSEIZE transect, the reference thermal model with a constant décollement position and no fluid circulation in the oceanic crust yields modeled surface heat flux more than 40 mW m^{-2} lower than observed on the incoming plate immediately seaward of the trench (Figure 7). The reference model is consistent with heat flux observations at the IODP boreholes on the margin (slightly lower than the scattered probe observations and BSR estimates for the margin wedge). Between 15 and 3.36 million years before present, insulated hydrothermal circulation in the basement aquifer (i.e., with no advective heat transport between the crustal aquifer and the ocean) homogenizes temperatures in the upper ocean crust. As in the generic insulated hydrothermal circulation cases, heat is extracted from under the margin wedge and transported into the crust seaward of the trench. As a result, relative to the reference model with no fluid flow, conductive heat flux across the seafloor is enhanced for crust approaching the subduction zone and heat flux across the margin wedge is reduced (Figure 7a). From 3.36 to 0.1 million years before present, the seamount acts
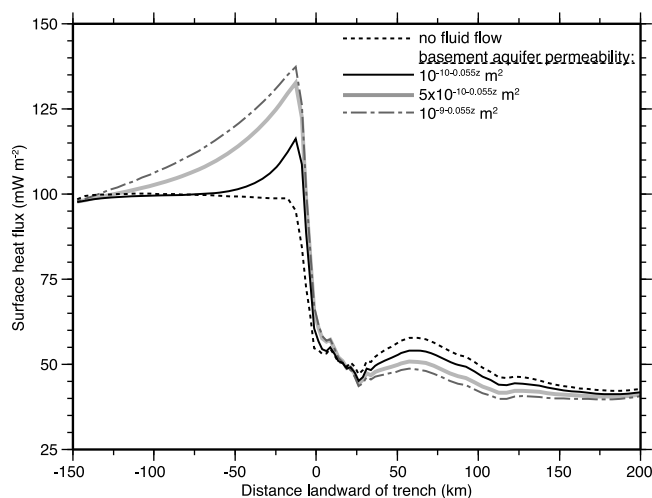
Figure 5. Effects of insulated hydrothermal circulation on surface heat flux. Dashed line is modeled surface heat flux with no hydrothermal circulation. Two solid lines and one dot-dashed line show modeled surface heat flux including thermal effects of fluid circulation in the oceanic crust basement aquifer. The redistribution of heat lowers surface heat flux on the margin wedge and causes a spike in heat flux in the trench. The magnitude of these anomalies increases with increasing aquifer permeability.

as a ventilator cooling the oceanic crust as it traverses from the seaward edge of the model to the trench. This reduces temperatures in the surrounding aquifer. The bulk of the thermal effects resulting from ventilated circulation are within 50 km of the seamount (Figures 7b and 7c). After seamount subduction, surface heat flux on the incoming plate and in the trench quickly recover to levels above those for the reference (no fluid flow) case, but lower than the insulated circulation case.

6. Discussion

[20] An abrupt shallowing of the décollement causing all incoming sediment to subduct has a small and narrowly focused effect on the surface heat flux pattern. The time required to warm the shallow subducting sediment is controlled by the thickness of the sediment layer and its thermal diffusivity. The 1400 m of sediment that switches from accretion to subduction with the change in décollement position is heated from below by normal heat conduction in the lithosphere and from above by frictional heating on the plate boundary fault. Thus, we estimate that ~25,000 years are required for heat conduction to penetrate this entire shallow sedimentary layer. Therefore, the cooling effect of the subduction of the shallow sediment is concentrated within 2.5 km landward of the trench with a convergence rate of 10 cm yr^{-1}; for a convergence rate of 2.5 cm yr^{-1}, most of the cooling

would occur in a region <1 km landward of the trench. The thermal effect is small and short lived.

[21] Hydrothermal circulation, either insulated or ventilated, has a larger effect on the thermal state of the margin than a shift in décollement position. Insulated hydrothermal circulation redistributes heat within the system, allowing some net cooling due to enhanced conductive heat flux across the seafloor on the incoming plate where sediment cover is thin. Over the estimated range of oceanic crust aquifer permeability [*Becker and Davis*, 2004; *Spinelli and Fisher*, 2004; *Hutnak et al.*, 2008], insulated hydrothermal circulation produces a potentially measurable surface heat flux anomaly seaward of the trench. Active ventilated hydrothermal circulation can extract large quantities of heat from oceanic lithosphere [e.g., *Fisher et al.*, 2003a; *Hutnak et al.*, 2008]. Such circulation can generate anomalously low surface heat flux in the trench [*Harris and Wang*, 2002; *Harris et al.*, 2010]. If seamount subduction induces a shift from ventilated to insulated hydrothermal circulation, the surface heat flux pattern transitions from anomalously cool to anomalously warm, approaching the pattern resulting from long-term insulated circulation. During this transition, the near-trench surface heat flux pattern can closely mimic the expected pattern with no fluid flow (Figure 6).

[22] Both thermal models with fluid circulation in the oceanic crust are more consistent with anomalously warm 20 Ma crust in the trench and a cool
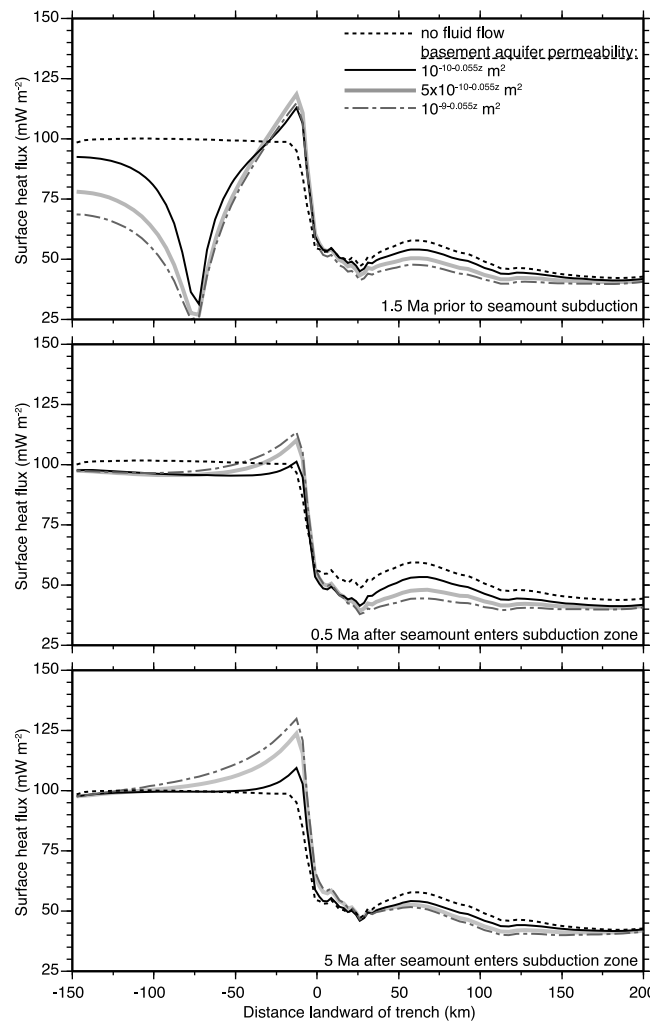
Figure 6. Effects of hydrothermal circulation transitioning from ventilated to insulated. Line types are the same as in Figure 5. Ventilated hydrothermal circulation cools the oceanic lithosphere locally. After subduction of the seamount eliminates the high-permeability conduit between the basement aquifer and the ocean, the system warms and approaches the thermal state achieved with insulated hydrothermal circulation.

margin wedge as observed in IODP boreholes than the reference model with no fluid flow (Figure 7). The elevated surface heat flux values on the incoming plate may reflect anomalously warm oceanic lithosphere throughout its history, not simply a focused increase in heat flux in the trench [*Harris et al.*, 2011]. In the Muroto transect, this scenario has been ruled out based on the progress of diagenetic reactions in the sediment on the incoming plate [*Spinelli and Underwood*, 2005]. In addition, most heat flux values far from the trench in Shikoku Basin are not indicative of anomalously hot oceanic lithosphere [*Yamano et al.*, 1984, 2003]. Additional surface heat flux observations on the incoming plate and/or sediment composition from ∼1 km depth on the incoming plate are required to test this hypothesis for the NanTroSEIZE transect. Taking a

synoptic view of controls on thermal state margin wide, we prefer the thermal models that include hydrothermal circulation; both the insulated and ventilated-then-insulated circulation models are consistent with the surface heat flux observations in the NanTroSEIZE transect. These models yield lower subduction zone temperatures than models with no fluid flow.

[23] The Nankai margin in the region of the NanTroSEIZE transect hosts a range of seismic behavior. The most recent large megathrust earthquake on the margin was the M8.1 Tonankai earthquake in 1944 [*Ando*, 1975]. Based on tsunami wave heights and onland deformation, the estimated rupture area on the plate boundary fault for this event extends from ∼20–45 km landward
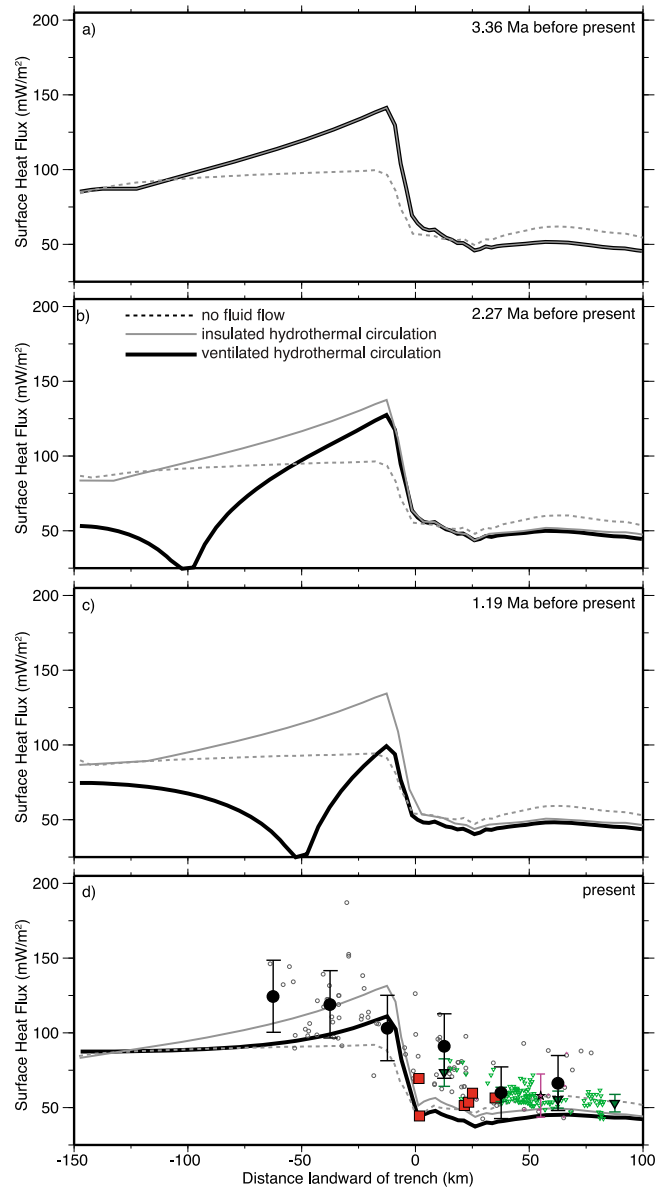
Figure 7. Surface heat flux observations and models in the NanTroSEIZE transect. Symbols are same as in Figure 2. (a) Modeled surface heat flux 3.36 million years before present, immediately prior to a seamount entering the model domain at 150 km seaward of the trench. Results (b) 2.27, (c) 1.19, and (d) 0 million years before present. Dashed gray lines are modeled surface heat flux with no fluid circulation. Solid gray lines are modeled surface heat flux with insulated hydrothermal circulation. Bold black lines are modeled surface heat flux with ventilated hydrothermal circulation.

of the trench [*Sagiya and Thatcher*, 1999]. This region coincides with the area strong coupling on the plate interface delineated by inversion of recent interseismic GPS observations [*Jin et al.*, 2007]. In addition to slip on the plate boundary fault, the 1944 earthquake rupture may have included slip on a large splay fault [*Baba et al.*, 2006]. Recently identified very low frequency earthquakes (VLFE) occur near the shallowest part of this same splay fault [*Obara and Ito*, 2005; *Obana and Kodaira*,

2009]. *Obana and Kodaira* [2009] suggest that these small low-frequency tremors indicate activity on the splay fault associated with high fluid pressure in the accretionary prism. Thus, seismic slip in this region, both during large megathrust events and small low-frequency tremors, can occur close to the seafloor (i.e., in regions with quite low temperatures). Nonvolcanic low-frequency tremors and areas of slow slip occur in a band downdip of the 1944 Tonankai rupture [*Obara and Hirose*, 2006].
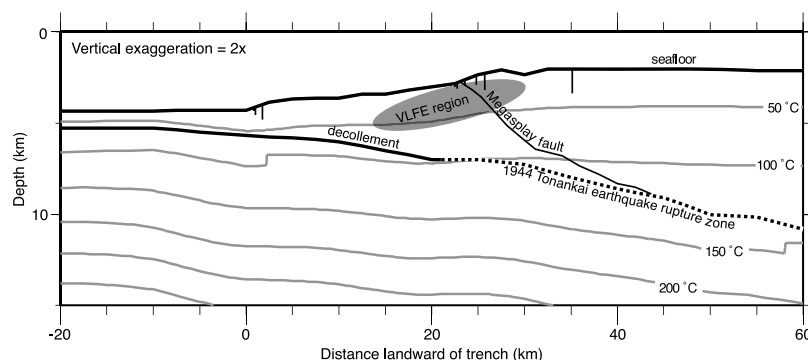
Figure 8. Temperature contours (50°C interval) in a vertical cross section along the NanTroSEIZE transect for the thermal model with ventilated-then-insulated hydrothermal circulation. Thin vertical lines extending below seafloor are IODP boreholes. Dashed line indicates the rupture area of the 1944 Tonankai earthquake. Shaded ellipse indicates area of very low frequency earthquakes in margin wedge.

[24] We use the results of our thermal models to estimate temperatures in the areas of various seismic activity in the NanTroSEIZE transect: the VLFE region in the accretionary prism, the megasplay fault, the rupture area of the 1944 Tohoku earthquake on the décollement, and the zone of episodic tremor and slip. Our preferred models estimate temperatures in the rupture area of the 1944 Tonankai earthquake ranging from 100°C to 295°C (Table 2). The greatest reduction in temperature, relative to a model with no fluid flow, is deep in the subduction zone; our preferred models yield temperatures in the region of episodic tremor and slip ∼70°C lower than a simulation with no fluid flow. Temperatures on the megasplay fault and in the region of very low frequency earthquakes in the accretionary prism are only slightly reduced by the effects of fluid circulation (Table 2).

7. Conclusions

[25] Seamounts approaching and entering a subduction zone may affect temperature distributions through their affects on the position of the subduction thrust and influence on patterns of hydrothermal circulation. A shift in décollement position to allow the subduction of an additional 1400 m of shallow sediment produces minor (<15 mW/m^2) cooling focused at the toe of the margin wedge. The approach toward the margin of a seamount acting as a conduit for fluid and heat between ocean and crustal aquifer cools the oceanic crust and allows heat mined from the subduction zone to vent to the ocean. In the wake of seamount subduction, the surface heat flux pattern may evolve from anomalously low to anomalously high heat flux in the trench. Early in this transition from ventilated to insulated hydrothermal circulation, the surface heat flux pattern may mimic the heat flux expected with no fluid flow. Anomalously high heat flux in the trench and scatter in heat flux values throughout the NanTroSEIZE transect suggest active fluid flow. The models most consistent with the heat flux observations include fluid circulation (either insulated or ventilated-then-insulated) in the ocean crust. Simulations with fluid circulation yield temperatures in the 1944 Tonankai rupture area 10°C–75°C lower than simulations without fluid circulation. Our preferred simulations yield temperatures in the region of episodic tremor and slip of ∼290°C–325°C, ∼70°C lower than a simulation without

Table 2. Modeled Temperatures (°C) in Various Fault Slip Zones

Simulation	Very Low Frequency Earthquakes[a]	Megasplay Fault[b]	1944 Tonankai Earthquake Rupture Area[c]	Episodic Tremor and Slip[d]
No fluid flow	0–40	0–165	120–365	365–390
Insulated hydrothermal Circulation	0–40	0–140	110–295	295–325
Ventilated hydrothermal Circulation	0–25	0–130	100–290	290–320

[a]*Obara and Ito* [2005]; *Obana and Kodaira* [2009].
[b]*Moore et al.* [2009].
[c]*Sagiya and Thatcher* [1999].
[d]*Obara and Hirose* [2006].

hydrothermal circulation. Accurate estimates of subduction zone temperatures are necessary to understand the locations of diagenetic and metamorphic reactions that may control physical properties within the seismogenic zone.

Acknowledgments

References

Ando, M. (1975), Source mechanisms and tectonic significance of historical earthquakes along the Nankai trough, *Japan, Tectonophysics*, *27*, 119–140, doi:10.1016/0040-1951(75)90102-X.

Baba, T., P. R. Cummins, T. Hori, and Y. Kaneda (2006), High precision slip distribution of the 1944 Tonankai earthquake inferred from tsunami waveforms: Possible slip on a splay fault, *Tectonophysics*, *426*, 119–134, doi:10.1016/j.tecto.2006.02.015.

Becker, K., and E. E. Davis (2004), In situ determinations of the permeability of the igneous oceanic crust, in *Hydrogeology of the Oceanic Lithosphere*, pp. 189–224, Cambridge Univ. Press, New York.

Bekins, B. A., A. M. McCaffrey, and S. J. Dreiss (1995), Episodic and constant flow models for the origin of low-chloride waters in a modern accretionary complex, *Water Resour. Res.*, *31*(12), 3205–3215, doi:10.1029/95WR02569.

Bessler, J. U., L. Smith, and E. E. Davis (1994), Hydrologic and thermal conditions at a sediment/basement interface: Implications for interpretation of field measurements at Middle Valley, *Proc. Ocean Drill. Program, Sci. Results*, *139*, 667–675.

Clift, P., and P. Vannucchi (2004), Controls on tectonic accretion versus erosion in subduction zones: Implications for the origin and recycling of the continental crust, *Rev. Geophys.*, *42*, RG2001, doi:10.1029/2003RG000127.

Davis, E. E., K. Wang, J. He, D. S. Chapman, H. Villinger, and A. Rosenberger (1997), An unequivocal case for high Nusselt-number hydrothermal convection in sediment-buried igneous oceanic crust, *Earth Planet. Sci. Lett.*, *146*, 137–150, doi:10.1016/S0012-821X(96)00212-9.

Dominguez, S., J. Malavieille, and S. E. Lallemand (2000), Deformation of accretionary wedges in response to seamount subduction: Insights from sandbox experiments, *Tectonics*, *19*(1), 182–196, doi:10.1029/1999TC900055.

Dumitru, T. A. (1991), Effects of subduction parameters on geothermal gradients in forearcs, with an application to Franciscan subduction in California, *J. Geophys. Res.*, *96*, 621–641, doi:10.1029/90JB01913.

Expedition 316 Scientists (2009a), Expedition 316 Site C0006, *Proc. Integr. Ocean Drill. Program*, 314/315/316, doi:10.2204/iodp.proc.314315316.134.2009.

Expedition 316 Scientists (2009b), Expedition 316 Site C0007, *Proc. Integr. Ocean Drill. Program*, 314/315/316, doi:10.2204/iodp.proc.314315316.135.2009.

Fisher, A. T. (2004), Rates and patterns of fluid circulation, in *Hydrogeology of the Oceanic Lithosphere*, edited by E. E. Davis and H. Elderfield, pp. 339–377, Cambridge Univ. Press, Cambridge, U. K.

Fisher, A. T., and M. W. Hounslow (1990), Transient fluid flow through the toe of the Barbados accretionary complex: Constraints from Ocean Drilling Program Leg 110 heat flow studies and simple models, *J. Geophys. Res.*, *95*(B6), 8845–8858, doi:10.1029/JB095iB06p08845.

Fisher, A. T., and C. G. Wheat (2010), Seamounts as conduits for massive fluid, heat, and solute fluxes on ridge flanks, *Oceanography*, *23*(1), 74–87, doi:10.5670/oceanog.2010.63.

Fisher, A. T., G. Zwart, and the Ocean Drilling Program Leg 156 Scientific Party (1996), Relation between permeability and effective stress along a plate-boundary fault, Barbados accretionary complex, *Geology*, *24*(4), 307–310, doi:10.1130/0091-7613(1996)024<0307:RBPAES>2.3.CO;2.

Fisher, A. T., C. A. Stein, R. N. Harris, K. Wang, E. A. Silver, M. Pfender, M. Hutnak, A. Cherkaoui, R. Bodzin, and H. Villinger (2003a), Abrupt thermal transition reveals hydrothermal boundary and role of seamounts within the Cocos Plate, *Geophys. Res. Lett.*, *30*(11), 1550, doi:10.1029/2002GL016766.

Fisher, A. T., et al. (2003b), Hydrothermal circulation across 50 km on a young ridge flank: The role of seamounts in guiding recharge and discharge at a crustal scale, *Nature*, *421*, 618–621, doi:10.1038/nature01352.

Hamamoto, H., M. Yamano, and S. Goto (2005), Heat flow measurement in shallow seas through long-term temperature monitoring, *Geophys. Res. Lett.*, *32*, L21311, doi:10.1029/2005GL024138.

Hamamoto, H., M. Yamano, S. Goto, M. Kinoshita, K. Fujino, and K. Wang (2011), Heat flow distribution and thermal structure of the Nankai subduction zone off the Ki-I Peninsula, *Geochem. Geophys. Geosyst.*, *12*, Q0AD20, doi:10.1029/2011GC003623.

Harris, R. N., and K. Wang (2002), Thermal models of the Middle America Trench at the Nicoya Peninsula, Costa Rica, *Geophys. Res. Lett.*, *29*(21), 2010, doi:10.1029/2002GL015406.

Harris, R. N., A. T. Fisher, and D. Chapman (2004), Seamounts induce large fluid fluxes, *Geology*, *32*(8), 725–728, doi:10.1130/G20387.1.

Harris, R. N., G. Spinelli, C. R. Ranero, I. Grevemeyer, H. Villinger, and U. Barckhausen (2010), Thermal regime of the Costa Rican convergent margin: 2. Thermal models of the shallow Middle America subduction zone offshore Costa Rica, *Geochem. Geophys. Geosyst.*, *11*, Q12S29, doi:10.1029/2010GC003273.

Harris, R. N., F. Schmidt-Schierhorn, and G. Spinelli (2011), Heat flow along the NanTroSEIZE transect: Results from IODP Expeditions 315 and 316 offshore the Kii Peninsula, Japan, *Geochem. Geophys. Geosyst.*, *12*, Q0AD16, doi:10.1029/2011GC003593.

Hill, I. A., et al. (1993), *Proceedings of the Ocean Drilling Program Initial Reports*, vol. 131, Ocean Drill. Program, College Station, Tex.

Hirose, F., J. Nakajima, and A. Hasegawa (2008), Three-dimensional seismic velocity structure and configuration of the Philippine Sea slab in southwestern Japan estimated by double-difference tomography, *J. Geophys. Res.*, *113*, B09315, doi:10.1029/2007JB005274.

Hutnak, M., A. T. Fisher, L. Zuhlsdorff, V. Spiess, P. Stauffer, and C. W. Gable (2006), Hydrothermal recharge and discharge guided by basement outcrops on 0.2–3.6 Ma seafloor east of the Juan de Fuca Ridge: Observations and numerical models, *Geochem. Geophys. Geosyst.*, *7*, Q07O02, doi:10.1029/2006GC001242.

Hutnak, M., A. T. Fisher, R. Harris, C. Stein, K. Wang, G. Spinelli, M. Schindler, H. Villinger, and E. Silver (2008), Large heat and fluid fluxes driven through mid-plate outcrops on ocean crust, *Nat. Geosci.*, *1*, 611–614, doi:10.1038/ngeo264.

Hyndman, R. D., and K. Wang (1993), Thermal constraints on the zone of major thrust earthquake failure: The Cascadia subduction zone, *J. Geophys. Res.*, *98*(B2), 2039–2060, doi:10.1029/92JB02279.

Hyndman, R. D., K. Wang, and M. Yamano (1995), Thermal constraints on the seismogenic portion of the southwestern Japan subduction thrust, *J. Geophys. Res.*, *100*(B8), 15,373–15,392, doi:10.1029/95JB00153.

Ike, T., G. F. Moore, S. Kuramoto, J.-O. Park, Y. Kaneda, and A. Taira (2008), Variations in sediment thickness and type along the northern Philippine Sea Plate at the Nankai Trough, *Isl. Arc*, *17*, 342–357, doi:10.1111/j.1440-1738.2008.00624.x.

Jin, H., T. Kato, and M. Hori (2007), Estimation of slip distribution using an inverse method based on spectral decomposition of Green's function utilizing Global Positioning System (GPS) data, *J. Geophys. Res.*, *112*, B07414, doi:10.1029/2004JB003378.

Kanaya, H., and S. Ishihara (1975), Uranium, thorium, afnd potassium contents of Japanese granitic rocks: A summary up to 1972, in *The Natural Radiation Environment II*, edited by J. A. S. Adams, W. M. Lowder, and T. F. Gesell, pp. 517–533, U.S. Energy Res. and Dev. Admin., Washington, D. C.

Kimura, G., E. J. Screaton, D. Curewitz, and the Expedition 316 Scientists (2008), NanTroSEIZE Project Stage 1 - Thrust Faults, *Integr. Ocean Drill. Program Prelim. Rep.*, *316*, doi:10.2204/iodp.pr.316.2008.

Kinoshita, M., T. Kanamatsu, K. Kawamura, T. Shibata, H. Hamamoto, and K. Fujino (2008), Heat flow distribution on the floor of Nankai Trough off Kumano and implications for the geothermal regime of subducting sediments, *JAMSTEC Rep. Res. Dev.*, *8*, pp. 13–28, Jpn. Agency for Mar.-Earth Sci. and Technol., Yokosuka.

Kinoshita, M., G. F. Moore, and Y. N. Kido (2011), Heat flow estimated from BSR and IODP borehole data: Implication of recent uplift and erosion of the imbricate thrust zone in the Nankai Trough off Kumano, *Geochem. Geophys. Geosyst.*, *12*, Q0AD18, doi:10.1029/2011GC003609.

Kummer, T. D., and G. A. Spinelli (2008), Hydrothermal circulation in subducting crust reduces subduction zone temperatures, *Geology*, *36*(1), 91–94.

Moore, G. F., et al. (2009), Structural and seismic stratigraphic framework of the NanTroSEIZE Stage 1 transect, *Proc. Integr. Ocean Drill. Program*, *314/315/316*, doi:10.2204/Iodp.proc.314315316.102.2009.

Mottl, M. J., et al. (1998), Warms springs discovered on 3.5 Ma oceanic crust, eastern flank of the Juan de Fuca Ridge, *Geology*, *26*(1), 51–54, doi:10.1130/0091-7613(1998)026<0051:WSDOMO>2.3.CO;2.

Obana, K., and S. Kodaira (2009), Low-frequency tremors associated with reverse faults in a shallow accretionary prism, *Earth Planet. Sci. Lett.*, *287*, 168–174, doi:10.1016/j.epsl.2009.08.005.

Obara, K., and H. Hirose (2006), Non-volcanic deep low-frequency tremors accompanying slow slips in the southwest Japan subduction zone, *Tectonophysics*, *417*, 33–51, doi:10.1016/j.tecto.2005.04.013.

Obara, K., and Y. Ito (2005), Very low frequency earthquakes excited by the 2004 off the Kii Peninsula earthquakes: A dynamic deformation process in the large accretionary prism, *Earth Planets Space*, *57*, 321–326.

Okino, K., Y. Shimakawa, and S. Nagaoka (1994), Evolution of the Shikoku Basin, *J. Geomagn. Geoelectr.*, *46*, 463–479, doi:10.5636/jgg.46.463.

Peacock, S. M. (1987), Thermal effects of metamorphic fluids in subduction zones, *Geology*, *15*, 1057–1060, doi:10.1130/0091-7613(1987)15<1057:TEOMFI>2.0.CO;2.

Peacock, S. M. (1996), Thermal and petrologic structure of subduction zones, in *Subduction: Top to Bottom*, *Geophys. Monogr. Ser.*, vol. 96, edited by G. E. Bebout et al., pp. 119–133, AGU, Washington, D. C., doi:10.1029/GM096p0119.

Saffer, D. M., and B. A. Bekins (1998), Episodic fluid flow in the Nankai accretionary complex: Timescale, geochemistry, flow rates, and fluid budget, *J. Geophys. Res.*, *103*(B12), 30,351–30,370, doi:10.1029/98JB01983.

Sagiya, T., and W. Thatcher (1999), Coseismic slip resolution along a plate boundary megathrust: The Nankai Trough, southwest Japan, *J. Geophys. Res.*, *104*(B1), 1111–1129, doi:10.1029/98JB02644.

Screaton, E., B. Carson, E. Davis, and K. Becker (2000), Permeability of a décollement zone: Results from a two-well experiment in the Barbados accretionary complex, *J. Geophys. Res.*, *105*(B9), 21,403–21,410, doi:10.1029/2000JB900220.

Seno, T., S. Stein, and A. E. Gripp (1993), A model for the motion of the Philippine Sea Plate consistent with NUVEL-1 and geological data, *J. Geophys. Res.*, *98*(B10), 17,941–17,948, doi:10.1029/93JB00782.

Spinelli, G. A., and A. T. Fisher (2004), Hydrothermal circulation within topographically rough basaltic basement on the Juan de Fuca Ridge flank, *Geochem. Geophys. Geosyst.*, *5*, Q02001, doi:10.1029/2003GC000616.

Spinelli, G. A., and M. B. Underwood (2005), Modeling thermal history of subducting crust in Nankai Trough: Constraints from in situ sediment temperature and diagenetic reaction progress, *Geophys. Res. Lett.*, *32*, L09301, doi:10.1029/2005GL022793.

Spinelli, G. A., and K. Wang (2008), Effects of fluid circulation in subducting crust on Nankai margin seismogenic zone temperatures, *Geology*, *36*(11), 887–890, doi:10.1130/G25145A.1.

Spinelli, G. A., and K. Wang (2009), Links between fluid circulation, temperature, and metamorphism in subducting slabs, *Geophys. Res. Lett.*, *36*, L13302, doi:10.1029/2009GL038706.

Spinelli, G. A., E. R. Giambalvo, and A. T. Fisher (2004), Sediment permeability, distribution, and influence on fluxes in oceanic basement, in *Hydrogeology of the Oceanic Lithosphere*, edited by E. E. Davis and H. Elderfield, pp. 151–188, Cambridge Univ. Press, New York.

Stein, C. A., and S. Stein (1994), Constraints on hydrothermal heat flux through the oceanic lithosphere from global heat flow, *J. Geophys. Res.*, *99*, 3081–3095.

Taira, A., et al. (1991), Proceedings of the Ocean Drilling Program, Initial Reports, vol. 131, Ocean Drilling Program, College Station, Tex.

Taira, A., et al. (2005), Nankai Trough Seismogenic Zone Site Survey, Philippine Sea, *Tech. Rep. 1*, Jpn. Agency Mar. Earth Sci. Technol., Yokohama, Japan.

Villinger, H., I. Grevemeyer, N. Kaul, J. Hauschild, and M. Pfender (2002), Hydrothermal heat flux through aged

Geochemistry Geophysics Geosystems G³

oceanic crust: Where does the heat escape?, *Earth Planet. Sci. Lett.*, *202*, 159–170, doi:10.1016/S0012-821X(02)00759-8.

von Huene, R., C. R. Ranero, W. Weinrebe, and K. Hinz (2000), Quaternary convergent margin tectonics of Costa Rica, segmentation of the Cocos Plate, and Central America volcanism, *Tectonics*, *19*, 314–334, doi:10.1029/1999TC001143.

Wada, I., and K. Wang (2009), Common depth of slab-mantle decoupling: Reconciling diversity and uniformity of subduction zones, *Geochem. Geophys. Geosyst.*, *10*, Q10009, doi:10.1029/2009GC002570.

Wang, K. (2004), Applying fundamental principles and mathematical models to understand processes and estimate parameters, in *Hydrogeology of the Ocean Lithosphere*, edited by E. E. Davis and H. Elderfield, pp. 376–413, Cambridge Univ. Press, New York.

Wang, K., and S. L. Bilek (2011), Do subducting seamounts generate or stop large earthquakes?, *Geology*, *39*(9), 819–822, doi:10.1130/G31856.1.

Wang, K., and J. He (1999), Mechanics of low-stress forearcs: Nankai and Cascadia, *J. Geophys. Res.*, *104*(B7), 15,191–15,205, doi:10.1029/1999JB900103.

Wang, K., R. D. Hyndman, and M. Yamano (1995), Thermal regime of the Southwest Japan subduction zone: Effects of age history of the subducting plate, *Tectonophysics*, *248*, 53–69, doi:10.1016/0040-1951(95)00028-L.

Wang, K., I. Wada, and Y. Ishikawa (2004), Stresses in the subducting slab beneath southwest Japan and relation with plate geometry, tectonic forces, slab dehydration, and damaging earthquakes, *J. Geophys. Res.*, *109*, B08304, doi:10.1029/2003JB002888.

Watanabe, T., D. Epp, S. Uyeda, M. Langseth, and M. Yasui (1970), Heat flow in the Philippine Sea, *Tectonophysics*, *10*, 205–224, doi:10.1016/0040-1951(70)90107-1.

Wheat, C. G., and A. T. Fisher (2008), Massive, low-temperature hydrothermal flow from a basaltic outcrop on 23 Ma seafloor of the Cocos Plate: Chemical constraints and implications, *Geochem. Geophys. Geosyst.*, *9*, Q12O14, doi:10.1029/2008GC002136.

Yamano, M., S. Honda, and S. Uyeda (1984), Nankai Trough: A hot trench?, *Mar. Geophys. Res.*, *6*, 187–203, doi:10.1007/BF00285959.

Yamano, M., M. Kinoshita, S. Goto, and O. Matsubayashi (2003), Extremely high heat flow anomaly in the middle part of the Nankai Trough, *Phys. Chem. Earth*, *28*, 487–497, doi:10.1016/S1474-7065(03)00068-8.